Journal of Visualized Experiments

Sub-unit-cell control of LaAlO3/SrTiO3 interfaces near the critical thickness -- Manuscript Draft--

Manuscript Number:	JoVE53413R5		
Full Title:	Sub-unit-cell control of LaAlO3/SrTiO3 interfaces near the critical thickness		
Article Type:	Invited Methods Article - JoVE Produced Video		
Keywords:	Aluminum Nitride (AIN) mask, Photolithography; RHEED; Field effect; LaAlO3/SrTiO3 Interfaces; metal-insulator transition; mobility; strain; Kondo effect		
Manuscript Classifications:	97.76.13: electrical transport properties in solids; 97.76.3: condensed matter physics; 97.76.31: thin films (theory, deposition and growth); 97.76.4: conductivity (solid state)		
Corresponding Author:	Changjian Li National University of Singapore Singapore, SINGAPORE		
Corresponding Author Secondary Information:			
Corresponding Author E-Mail:	changjian_li@u.nus.edu		
Corresponding Author's Institution:	National University of Singapore		
Corresponding Author's Secondary Institution:			
First Author:	Changjian Li		
First Author Secondary Information:			
Other Authors:	Shengwei Zeng		
	Weiming Lü		
	Ariando Ariando		
	Thirumalai Venkatesan		
Order of Authors Secondary Information:			
Abstract:	The two-dimensional electron gas (2DEG) at the interface between a polar (LaAlO3 or LAO) and non-polar (SrTiO3 or STO) insulating oxide offers opportunities to develop multifunctional devices. The prospect of this interface will depend on both its performance compared to existing technologies and its ability to integrate with CMOS technology. As a measure for the 2DEG electronic quality, the carrier density and mobility are commonly used, and they strongly relate to the quality of the hosting material and interface. A good understanding of the material growth and interface formation therefore would be required to be able to control and tune the electron density and mobility. Using pulsed laser deposition with in-situ reflection high energy electron diffraction (RHEED), we demonstrate the control of LAO growth at sub-unit-cell precision. While it is commonly observed that the LAO/STO shows a metal-to-insulator transition (MIT) at around 3 to 4 unit-cells (uc) of LAO, our results demonstrate that it occurs precisely at 3.65 uc (with the last LAO layer having only 65% coverage). Near this critical value, we further show that the electron mobility is sensitive to the degree of the surface coverage, carrier density (which can be varied by back gating) and magnetic scattering (which is seen at high carrier concentrations). In this paper, the sample fabrication and characterization process are elaborated and we propose that this process might also be applicable for growing other (oxide) interfaces.		
Author Comments:	Hope the filming can be done before June 1st 2015 because I will graduate soon.		
Additional Information:			
Question	Response		

If this article needs to be "in-press" by a certain date to satisfy grant requirements, please indicate the date below and explain in your cover letter.	
If this article needs to be filmed by a certain date to due to author/equipment/lab availability, please indicate the date below and explain in your cover letter.	05-29-2015

Cover Letter

The Editor

JoVE,

Dear Editor,

We would like to submit the manuscript, Controlled fractional unit cell growth of LaAlO₃/SrTiO₃ interfaces near the critical thickness and its scattering properties by C. J. Li et al., for consideration in JoVE.

The two dimensional electron gas (2DEG) generated at the LaAlO₃/SrTiO₃ (LAO/STO) interface has been a very exciting development over the last decade and the potential for oxide electronic devices based on these interfaces would require a clear understanding of the electronic transport properties at these interfaces and our ability to manipulate them at will.

For this purpose, we developed a standard protocol for controlled fractional unit cell growth of LAO, patterning the 2DEG and characterization of the patterned 2DEG. Using these techniques, we have successfully identified the exact critical thickness for the metal-insulator transition of 3.65 uc. Further, the carrier carrier scattering, strain and Kondo induced scattering are three major scattering mechanisms affecting the transport properties of LAO/STO interfaces. In this paper, we illustrate the detailed procedures of the experiments to make it available to wide research community and applicable to other oxide interface systems.

We feel techniques described in this paper are simple and general enough and will lead to a broad interest in general oxide thin film fabrication and characterization community and hence eminently suited for publication in JoVE.

Sincerely,

Changjian Li and T. Venkatesan.

```
1
      TITLE:
 2
      Sub-unit-cell control of LaAlO<sub>3</sub>/SrTiO<sub>3</sub> interfaces near the critical thickness
 3
 4
      AUTHORS:
 5
      Li, Changjian
 6
      NUSNNI-Nanocore
 7
      National University of Singapore
 8
      Singapore, Singapore
 9
10
      National University of Singapore Graduate School for Integrative Sciences and Engineering
11
      (NGS)
12
      Singapore, Singapore
13
      Changjian li@u.nus.edu
14
15
      Zeng, Shengwei
      NUSNNI-Nanocore
16
17
      National University of Singapore
18
      Singapore, Singapore
19
      nnizs@nus.edu.sg
20
21
      Lü, Weiming.
22
      NUSNNI-Nanocore
23
      National University of Singapore
24
      Singapore, Singapore
25
      elelwm@nus.edu.sg
26
27
      Ariando
28
      NUSNNI-Nanocore
29
      National University of Singapore
30
      Singapore, Singapore
31
32
      Department of Physics
33
      National University of Singapore
34
      Singapore, Singapore
35
      ariando@nus.edu.sg
36
37
      Venkatesan, Thirumalai. V.
38
      NUSNNI-Nanocore
39
      National University of Singapore
40
      Singapore, Singapore
41
42
      National University of Singapore Graduate School for Integrative Sciences and Engineering
43
      (NGS)
44
      Singapore, Singapore
```

45

46 Department of Physics

47 National University of Singapore

48 Singapore, Singapore

49 venky@nus.edu.sg

50 51

CORRESPONDING AUTHOR:

52 Lü, Weiming

elelwm@nus.edu.sg

53 54

55 Venkatesan, Thirumalai. V.

56 <u>venky@nus.edu.sg</u>

57 58

59

60

KEYWORDS:

Aluminum Nitride (AIN) mask, photolithography, reflection high energy electron diffraction (RHEED), field effect, LaAlO₃/SrTiO₃ interface, metal-insulator transition, mobility, strain, Kondo effect

61 62 63

64

65

66

SHORT ABSTRACT:

We present a standard protocol for growing sub-unit-cell LaAlO₃ near the critical thickness of the LaAlO₃/SrTiO₃ metal-to-insulator transition using pulsed laser deposition with *in-situ* reflection high energy electron diffraction (RHEED). Electric field effect measurements of these sub-unit-cell interface samples reveal different scattering mechanisms.

67 68 69

70

71

72

73

74

75

76

77

78

79

80

81

82

83

84

85

LONG ABSTRACT:

The two-dimensional electron gas (2DEG) at the interface between a polar (LaAlO₃ or LAO) and non-polar (SrTiO₃ or STO) insulating oxide offers opportunities to develop multifunctional devices. The prospect of this interface will depend on both its performance compared to existing technologies and its ability to integrate with complementary metal-oxidesemiconductor (CMOS) technology. As a measure for the 2DEG electronic quality, the carrier density and mobility are commonly used, and they strongly relate to the quality of the hosting material and interface. A good understanding of the material growth and interface formation therefore would be required to be able to control and tune the electron density and mobility. Using pulsed laser deposition with in-situ reflection high energy electron diffraction (RHEED), we demonstrate the control of LAO growth at sub-unit-cell precision. While it is commonly observed that the LAO/STO shows a metal-to-insulator transition (MIT) at around 3 to 4 unitcells (uc) of LAO, our results demonstrate that it occurs precisely at 3.65 uc (with the last LAO layer having only 65% coverage). Near this critical value, we further show that the electron mobility is sensitive to the degree of the surface coverage, carrier density (which can be varied by back gating) and magnetic scattering (which is seen at high carrier concentrations). In this paper, the sample fabrication and characterization processes are elaborated and we propose that these processes are also applicable for growing other (oxide) interfaces.

868788

INTRODUCTION:

Since the first report by Ohtomo and Hwang¹, two-dimensional electron gas (2DEG) at the interface between a polar insulator LaAlO₃ (LAO) and non-polar insulator SrTiO₃ (STO) has attracted extensive research in order to understand its origin²⁻⁵ and explore its properties⁶⁻⁸ and potential applications. To exploit the 2DEG in electronic devices, the ability to control and tune its electronic properties is a prerequisite. A good understanding on the 2DEG scattering mechanism is thus required, which directly relates to the interface carrier density and mobility.

95 96

97

98

99

100101

102

103

104

105

106

107

108

109

110

111

112

113

114

115116

94

89 90

91

92 93

> It is generally observed that the insulator-to-metallic transition at the LAO/STO interface occurs when the LAO thickness is around 3-4 unit-cells (uc). However, the observed values of carrier density and mobility at the critical thickness tend to vary from one report to another, and this might be due to that the precise LAO thickness is less controlled. In previous studies¹⁵, the top (last) LAO layer during deposition is usually assumed to be an integer of unit cells, i.e. a layer with a complete coverage. In this paper, we established a method to precisely control the growth of LAO layer with sub-unit-cell precision near the critical thickness of between 3 and 4 uc by monitoring the RHEED intensity oscillation during the LAO growth using PLD. In addition, we developed a technique to create micron patterns of the 2DEG based on lithographically patterned amorphous AIN layer before the growth of the LAO polar layer. The motivation is that a good recipe to chemically etch oxide layer is not yet established while the ion-beam etching technique may result in defects formation on the STO surface that may lead to an unwanted surface conductivity. Furthermore, an ion beam etching facility is not always available in every research lab. Another alternative is a lift-off process. However, as the deposition temperature to produce a crystalline LAO is relatively high (650 °C and above), a normal photoresist cannot withstand the high temperature. We have developed a process to pattern amorphous AIN as a replacement for the photoresist, and in this case a negative image of the desired pattern has to be produced. The use of AIN as a mask allows the subsequent deposition of LAO to be performed at high temperatures. The area uncovered by AIN defines the final pattern of our structures and the deposition of LAO directly on this area produces interface conductivity, while the LAO deposited on AIN remain insulating. This process allows patterning of the 2DEG without complicated and damaging etching process.

117118119

120

121

122

123

124

125

126

The carrier density and mobility of the samples were characterized using Hall effects, showing that the 2DEG starts to emerge when the LAO thickness is 3.65 uc (65% coverage of the fourth LAO layer) and the 2DEG mobility is sensitive to the surface coverage above this critical value. In order to understand the relation between carrier density and mobility, the 2DEG density was tuned using electric field with the STO substrate as the dielectric. The Hall and field effect data show that the mobility depends on the coverage of the top LAO layer and carrier density, indicating that it is governed by various scattering mechanisms including carrier-carrier, strain induced defect, and magnetic (only observed at high carrier concentration) scatterings. These results provide guidance in tuning the 2DEG and designing future oxide electronics.

127128129

PROTOCOL:

130

1. Substrate preparation

131132

133 1.1 Obtain commercially available single- or double-side polished single-crystal STO (001) substrates of 0.5 mm thick and 5x5 mm² surface area.

135

1.2 Immerse and ultrasonically soak the as-received STO substrates in 0.1 L deionized water for 10 min. The topmost layer of SrO domains will form Sr-hydroxide complex, which can be dissolved in acidic solution.

139

1.3 Immediately dip the substrates into 50 mL buffered hydrofluoric acid (BHF) solution and ultrasonically soak for 30 s. Subsequently, rinse the substrates with deionized water and dry them with nitrogen spray. The BHF will selectively etch away the SrO domains, producing practically perfect TiO₂ termination on the STO surface.

144

1.4 To remove the remnants of the previous treatments and facilitate recrystallization, 146 anneal the substrates in a furnace in an atmospheric pressure, with the following steps; heat up 147 to 950 °C at a rate of 5 °C/min, keep at 950 °C for 1.5 hours, and cool down to room 148 temperature at a rate of 3 °C/min.

149

1.5 Perform atomic force microscopy (AFM) in a tapping mode with a scanning rate of 1 Hz over an area of $3\times3~\mu\text{m}^2$ in order to characterize the surface morphology according to manufacturer's protocol.

153154

1.5.1. Use the built-in AFM software to open and analyze the obtained image files. If necessary, subtract any background and measurement artifacts. A single TiO₂ terminated surface should show clear atomic terraces.

156157

155

1.5.2. Determine the root mean square (rms) roughness of the surface and the width and
 height (should correspond to the lattice constant of STO of around 0.4 nm) of the terraces.
 Export the processed images into .jpg file. Figure 1 shows the evolution of the STO surface
 morphology captured after each treatment step.

162163

2. Photolithography

164165

166 167 2.1 Load and secure a BHF treated STO substrate onto a spin coater, coat with 0.5 mL poly(methyl methacrylate) (PMMA) photoresist, and immediately spin at 3000 rpm for 1 min. Unload the substrate from the spin coater and bake it on a hot plate at 120 °C for 1 min. Repeat this procedure for all other substrates.

168 169

170 2.2 Load and secure the substrate in the UV mask aligner. Align the pre-designed mask (with 171 Hall bar structures) on the sample and expose for 8 s. The Hall bar mask is manufactured using 172 laser writing process with the bar dimension of 160 μ m in length and 100 μ m in width (see 173 Figure 2a). Repeat this procedure for all other substrates.

174

Unload the substrate from the mask aligner and immerse in PMMA developer for 1 min.
The positive image of the Hall bar will be obtained on the surface. Repeat this procedure for all

177 other substrates.

3. AIN sacrificial mask deposition

3.1 Secure the aluminum nitride (AIN) target on a Pulse Laser Deposition (PLD) target holder, and glue the backside of one of the STO on a substrate holder using ~2 mL silver paint and place the holder on a hot plate for ~10 min at 100 °C to dry the silver paint and allow a good thermal contact between the holder and substrate. Load both the target and substrate holders into the PLD deposition chamber.

3.2 Adjust the substrate-target distance to 7 cm and wait for the base pressure of the PLD chamber to reach at least 1×10^{-7} Torr.

190 3.3 After the expected base pressure is obtained, introduce pure oxygen into the deposition chamber and adjust its flow until a stable pressure of ~1 × 10⁻⁶ Torr is achieved.

Align the Laser optics, adjust the Laser power and to obtain an energy fluence of 1.5 J/cm² on the target surface, and set the repetition rate to 5 Hz. Rotate and raster the target during laser ablation to uniformly ablate the target surface area.

3.5 Start a predeposition by ablating the AIN target with the laser with the target shutter closed to clean the AIN target. After 5 min predeposition, open the target shutter to start the deposition.

3.5.1. To produce a uniform layer, rotate the substrate during laser ablation. After a 30 min deposition to obtain 100 nm thick AIN, stop the deposition by switching-off the laser. The growth rate of AIN has been previously calibrated. An amorphous AIN layer is produced and it fully covers the previously structured photoresist.

3.6 Stop all target and substrate rastering and rotation, and switch-off the oxygen flow. Unload the substrate from the chamber.

3.7 Immerse the substrate into a beaker filled with ~50 mL acetone and ultrasonically soak for 1 min. Rinse the substrate with deionized water and make sure photoresist is completely removed.

213 3.8 Observe the obtained Hall bar pattern under an optical microscope; a representative pattern is shown in Figure 2a. Repeat the cleaning process if necessary.

4. LAO Film deposition

4.1 Using the same process as 3.1, load a LAO single crystal target and the STO substrate obtained from section 3 into the PLD chamber.

221 4.2 Wait for the base pressure of the chamber to reach 1×10^{-7} Torr.

222

223 4.3 Introduce pure oxygen into the deposition chamber and adjust its flow until a stable 224 pressure of 1×10^{-3} Torr is achieved.

225

4.4 Turn on the RHEED electron gun and set the voltage to 25 kV and filament current to 1.5
 A. Open the valve between the RHEED and deposition chamber. Turn on the RHEED CCD
 camera.

229230

231

232

4.5 Adjust the z-position and rotation-angle of the substrate with respect to the electron beam until a good RHEED pattern is observed on the CCD camera. An example of a good RHEED pattern is shown in Figure 3 for different steps for thin film growth. The z-position is ~86 and the rotation angle is not fixed.

233234235

4.6 Heat up the substrate heater at 15 °C/min until it reaches and stabilizes at 900 °C (corresponding to a substrate temperature of about 750 °C). Wait for about 5 minutes.

236237238

239

4.7 Repeat step 3.4 and set Laser fluence at 1.5 J/cm² and repetition rate at 2 Hz, and perform predeposition for 5 mins. Meanwhile, observe the RHEED pattern and, if necessary, adjust again the sample position to get a good RHEED pattern (see Figure 3).

240241242

243

244

4.8 Start deposition by opening the target shutter. Using the RHEED software, monitor the intensity of the specular spot (specified in Figure 3) of the image on the CCD camera. The software will display and record a real time evolution of the spot intensity, showing a periodic oscillation. Figure 4c and 4d show examples of the intensity oscillation.

245246247

248

4.9 Determine the periodicity of the oscillation by counting the peak-to-peak duration. One period corresponds to one unit-cell (~0.4 nm) growth of LAO. The growth rate in our chamber with the deposition parameters described above is 0.025 uc/sec.

249250251

252

4.10 Based on the growth rate, stop the laser at the desired LAO thickness. For example, to obtain 3.50 uc samples, stop the laser at 140 sec mark. Figure 4 shows an example of the subunit-cell growth control process.

253254255

4.11 Stop all target and substrate rastering and rotation, and set the substrate temperature to 25 °C at 10 °C/min while keeping the pressure the same as the deposition pressure.

256257

258 4.12 When the sample temperature reaches 100 °C or lower, switch off the oxygen flow.
259 Unload the sample from the chamber.

260

4.13 Anneal the sample by heating it up to 600 °C at 10 °C/min in a furnace with an oxygen flow at 0.5 bar. Keep the sample in the furnace for 1 hour and subsequently cool it down to room temperature at 10 °C/min. This step removes oxygen vacancies from the sample and minimizes their contribution to the conductivity.

265
266 4.14 Repeat steps 4.1 to 4.13 for deposition of different LAO thicknesses (3.5, 3.65, 3.8 and 4 uc).

5. Atomic force microscopy

271 5.1 Load the sample onto the AFM sample stage.

5.2 Load the AFM cantilever and make an adjustment to the laser and photodiode suitablefor scanning in a tapping mode.

276 5.3 Scan the sample surface with a scanning rate of 1 Hz and scanning area of $3 \times 3 \mu m^2$.

278 5.4 Analyze the AFM images with the same method discussed in section 1.5. Some obtained 279 images are shown in Figure 4.

281 5.5 Repeat steps 5.1 to 5.4 for other samples with different thicknesses (3.5, 3.65, 3.8 and 4 uc).

6. Hall and electric field effects

Paste a sample on a copper plate by uniformly covering the backside of the sample with approximately 2 mL silver paint. This ensures a good electrical contact between the copper plate and the substrate and allows electric fields to be applied to the STO substrate through the copper plate for the field effect measurement.

6.2 Using approximately 2 mL low temperature grease, secure the copper plate on a sample holder suitable for the physical properties measurement system (PPMS) with the sample surface facing up.

6.3 Form electrical connections between the sample and sample holder by Al wire for each respective electrical pads using ultrasonic wire bonder with a bonding power of 270 W and duration of 30 msec. The connection layout for the samples is shown in Figure 2b.

6.4 Load the sample holder into the PPMS chamber and stabilize the temperature by inputting a set point of 300 K. Set the measurement (driving) current to 1 μ A and the potential range of the source meter for the gate voltage to 50 V.

6.5 Switch on the applied magnetic field and sweep the field from 0 to 9 T while measuring the longitudinal or perpendicular (Hall) resistance through their respective potential connections. (Figure 2b)

6.6 Observe any leakage current through the bottom STO gate through a multimeter during application of a gate voltage. The leakage current must be less than 10 nA.

309

310 6.7 Repeat step 6.4 for different applied gate voltages (from -50 V to 50 V with a 10 V step) 311 and for different temperatures (300, 200, 100, 50, 20, 10, 5 and 2 K).

312

313 6.8 Repeat steps 6.1 to 6.6 for other samples with different thicknesses (3.5, 3.65, 3.8 and 4 314 uc).

315

316 6.9 Analyze the resistance-magnetic field dependence curves and calculate the carrier density and mobility of the samples by using the following relations:

317

- $n = -\frac{1}{e \cdot Hall \ slope}$ (1) 318
- $\mu = \frac{L}{RW} \cdot \frac{1}{ne} = \frac{L}{RW} \cdot (-Hall\ slope) \ (2),$ 319
- where n and μ are carrier density and mobility, respectively, R is the linear resistance, Hall slope 320 321 is the gradient of the Hall resistance versus magnetic field, L and W are the length (160 µm) and 322 the width (100 μm) of the Hall bar, respectively, and e is the elementary charge.

323

324 The magnetoresistance (MR) is defined as $MR(B) = R(B) - R(0) / R(0) \times 100 \%$, where R(B) is the 325 resistance at an applied magnetic field B and R(0) is the resistance at zero magnetic field.

326 327

REPRESENTATIVE RESULTS:

328 The substrate preparation process greatly affects the quality of STO surfaces. Figure 1 shows 329 the evolution of the surface morphology before and after BHF and thermal treatment. The as-330 received substrates show a very smooth surface without atomic terraces. After BHF treatment, 331 terraces start to form but with diffusive edges. The terrace edges become sharp only after 332 thermal annealing, indicating the formation of atomically flat surface ideal for layer-by-layer 333 growth (step 2).

334

335 Figure 2a shows a Hall bar that is defined by depositing an amorphous AIN mask. There are four 336 of such structures on every 5x5 mm² area of the substrate. After LAO deposition, the Hall bar 337 region (which is not covered by AIN) becomes conducting while the rest remains insulating. 338 Figure 2b shows a schematic of the electrical connections for the Hall effect measurement 339 including a voltage gatefor applying electric field.

340 341

342

The thin film growth is monitored by an in-situ RHEED. Figure 3 shows a typical RHEED pattern at room temperature (a) and at the deposition temperature before (b) and after (c) the deposition.

343 344 345

346

347

Following the above protocol, we have successfully fabricated LAO/STO interfaces with a LAO thickness varying from 3.5 to 4 uc. The differences in morphology between 3 and 3.5 uc LAO grown on STO are shown in Figure 4a and 4b and the RHEED oscillations during the LAO growth for 3.6 and 3.8 uc are shown in Figure 4c and 4d, respectively.

348 349

350 The resistance data of different samples with a LAO thickness increased in a sub-unit-cell step between 3 and 4 uc provide us a more precise critical thickness (3.65 uc) of the LAO/STO 351

insulator-to-metallic transition. Furthermore, the carrier density and mobility can be extracted from the field effect data, through equations (1) and (2), for different LAO thicknesses at different gate voltages, providing us the density dependence of the carrier mobility. As depicted in Figure 5, this dependence suggests that the carrier-carrier scattering plays an important role at the LAO/STO interface.

Figure 1. Evolution of the substrate surface morphology during BHF treatment. AFM images of (a) an as-received, (b) a BHF treated, and (c) a BHF treated and thermally annealed STO substrate. It shows selective etching and recrystallization processes makes atomically flat surfaces.

Figure 2. Hall bar and Hall effect measurement. (a) Optical microscopy images of the Hall bar defined by a lithographically patterned amorphous AIN layer. The "6" shape mark is at the back of the substrate. (b) The wiring layout for the Hall and electric field effect.

Figure 3. Evolution of RHEED patterns during the LAO growth: (a) before deposition at room temperature, (b) before deposition at 900 °C and (c) after deposition at 900 °C, respectively. The red oval enclosed spot is the spot which intensity is monitored.

Figure 4: Sub-unit-cell control of the LAO growth on a STO substrate. AFM images of a (a) 3 uc and (b) 3.5 uc LAO sample obtained by scanning the sample surface over the Hall bar area. The 3 uc sample shows atomically smooth terraces, while the 3.5 uc sample shows island formations on the terraces. (c) and (d) show RHEED oscillations during the growth of 3.6 and 3.8 uc of LAO, respectively.

Figure 5: Density dependence of the carrier mobility at 2 K for samples with different LAO thicknesses.

DISCUSSION:

The sample fabrication protocol described above allows sub-unit-cell control of LAO growth on a STO substrate in LAO/STO heterojunctions as shown in Figure 4. The growth control relies on the *in-situ* RHEED monitoring in a PLD system, and this protocol might be applicable to other material systems which exhibit a layer-by-layer growth mode. For materials having other growth modes, such as island growth, there is no periodic oscillation of the RHEED intensity expected, and thus sub-unit-cell control cannot be achieved with this method.

The introduction of AIN as a sacrificial mask is a reliable and robust technique to create submicron patterns on oxide heterostructures. This technique is much simpler and avoids the possibility of a defect formation under the etched oxide layer, which is commonly observed during ion-milling and may introduce a redundant conducting surface. The approach here would be applicable to create sub-micron structures in other (oxide) interfaces and heterojunctions.

The electric field effect is a powerful technique to continuously tune carrier density (see Figure

5 where carrier density is tuned from $1 \times 10^{13} - 5 \times 10^{13}$ cm⁻²) of a material system without changing its structural and chemical composition. In this study, electric field effects using a back gate configuration with STO as the dielectric is utilized. Even though a large gate voltage is typically needed, the main advantage of such a configuration is that the STO substrate exhibits a large dielectric constant, in particular at low temperatures below 60 K, allowing a carrier modulation of up to 5×10^{14} cm⁻². A larger carrier modulation of up to 1×10^{15} cm⁻² with a low gate voltage (of a few volts) can now be achieved by utilizing ionic liquid in an electronic double layer transistor (EDLT) configuration, a technique that is becoming popular nowadays.

In this protocol, the critical step is the photolithography process. The UV exposure time and development time of the photoresist should be carefully controlled. If it is underdeveloped, there is some photoresist residual left on the substrate. As a result, acetone will lift off a larger area than the desired Hall bar pattern, causing the conducting path to not be defined properly. The poorly defined conducting channels affect the transport measurement results. To solve this problem, exposure and develop time have to be optimized experimentally.

In conclusion, the experimental protocol discussed in this paper allows a sub-unit-cell control of the LAO layer and sub-micron patterning in the LAO/STO interfaces. The electrical characterization of samples prepared by following this protocol provide a better understanding on the scattering mechanism of the 2DEG in the vicinity of the metal-to-insulator transition. This protocol should be applicable to other (oxide) interface systems.

ACKNOWLEDGMENTS:

This work is supported by the Singapore National Research Foundation (NRF) under the
Competitive Research Programs (CRP) "Tailoring Oxide Electronics by Atomic Control" (CRP
Award No.NRF2008NRF-CRP002-024) and "New Approach To Low Power Information Storage:
Electric-Field Controlled Magnetic Memories" (CRP Award No. NRF-CRP10-2012-02).

DISCLOSURES:

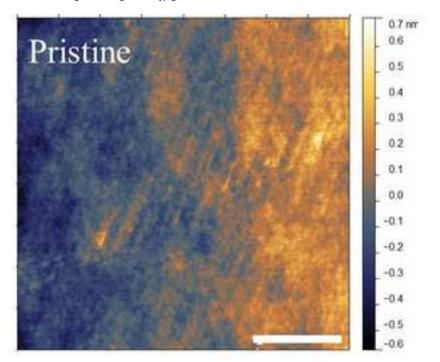
The authors have nothing to disclose.

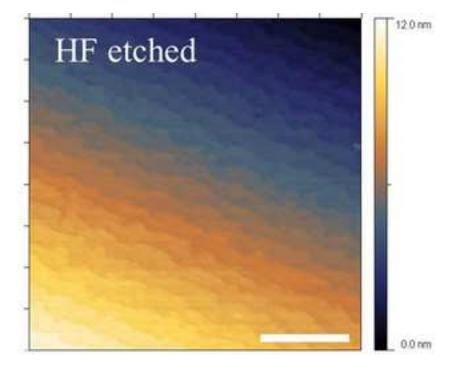
REFERENCES

- Ohtomo, A. & Hwang, H. Y. A high-mobility electron gas at the LaAlO3/SrTiO3 heterointerface. *Nature* **427**, 423-426, doi: 10.1038/nature02308 (2004).
- 430 2 Nakagawa, N., Hwang, H. Y. & Muller, D. A. Why some interfaces cannot be sharp. *Nat* 431 *Mater* **5**, 204-209, doi: 10.1038/nmat1569 (2006).
- 432 3 Popović, Z. S., Satpathy, S. & Martin, R. M. Origin of the Two-Dimensional Electron Gas 433 Carrier Density at the LaAlO₃ on SrTiO₃ Interface. *Phys. Rev. Lett.* **101** (25), 256801, doi: 434 10.1103/PhysRevLett.101.256801 (2008).
- 435 4 Pentcheva, R. & Pickett, W. E. Avoiding the Polarization Catastrophe in LaAlO₃
 436 Overlayers on SrTiO₃ (001) through Polar Distortion. *Phys. Rev. Lett.***102** (10), 107602,
 437 doi: 10.1103/PhysRevLett.102.107602 (2009).
- Willmott, P. R. *et al.* Structural Basis for the Conducting Interface between LaAlO₃ and SrTiO₃. *Phys. Rev. Lett.* **99** (15), 155502, doi: 10.1103/PhysRevLett.99.155502 (2007).

440 441 442	6	Liu, Z. Q. et al. Origin of the Two-Dimensional Electron Gas at LaAlO $_3$ /SrTiO $_3$ Interfaces: The Role of Oxygen Vacancies and Electronic Reconstruction. <i>Phys. Rev. X</i> 3 (2), 021010, doi: 10.1103/PhysRevX.3.021010 (2013).
443	7	Thiel, S., Hammerl, G., Schmehl, A., Schneider, C. W. & Mannhart, J. Tunable Quasi-Two-
444		Dimensional Electron Gases in Oxide Heterostructures. <i>Science</i> 313 , 1942-1945, doi:
445		10.1126/science.1131091 (2006).
446	8	Brinkman, A. et al. Magnetic effects at the interface between non-magnetic oxides. Nat
447		<i>Mater</i> 6 , 493-496, doi: 10.1038/nmat1931 (2007).
448	9	Reyren, N. et al. Superconducting Interfaces Between Insulating Oxides. Science 317,
449		1196-1199, doi: 10.1126/science.1146006 (2007).
450	10	Basletic, M. et al. Mapping the spatial distribution of charge carriers in LaAlO3/SrTiO3
451		heterostructures. Nat Mater 7, 621-625, doi: 10.1038/nmat2223 (2008).
452	11	Li, L., Richter, C., Mannhart, J. & Ashoori, R. C. Coexistence of magnetic order and two-
453		dimensional superconductivity at LaAlO ₃ /SrTiO ₃ interfaces. <i>Nat Phys</i> 7 , 762-766, doi:
454		10.1038/nphys2080 (2011).
455	12	Bert, J. A. et al. Direct imaging of the coexistence of ferromagnetism and
456		superconductivity at the LaAlO ₃ /SrTiO ₃ interface. <i>Nat Phys</i> 7 , 767-771, doi:
457		10.1038/nphys2079 (2011).

Figure 1 Click here to download Figure: Figure 1.jpg





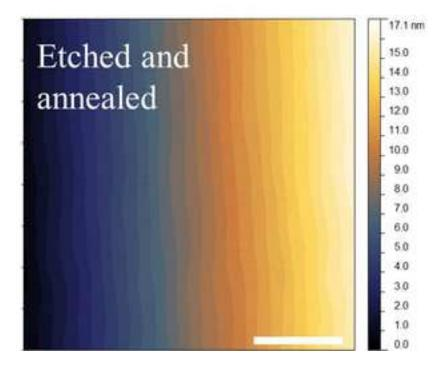


Figure 2 Click here to download Figure: Figure 2.jpg

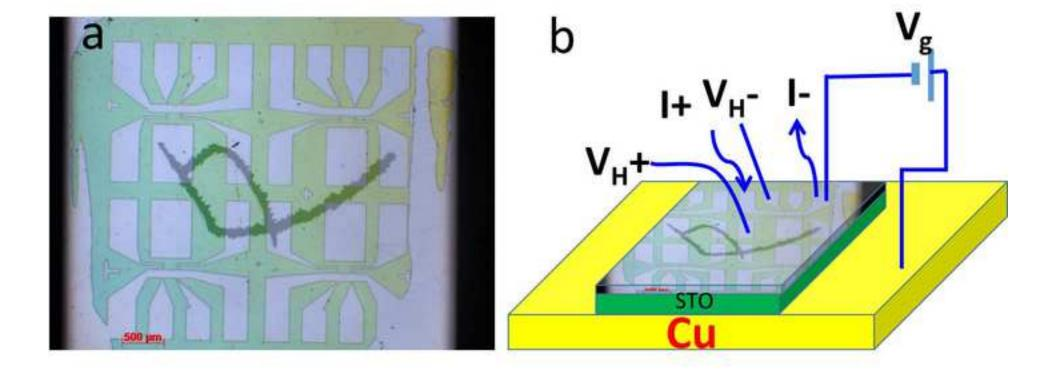


Figure 3
Click here to download Figure: Figure 3.jpg

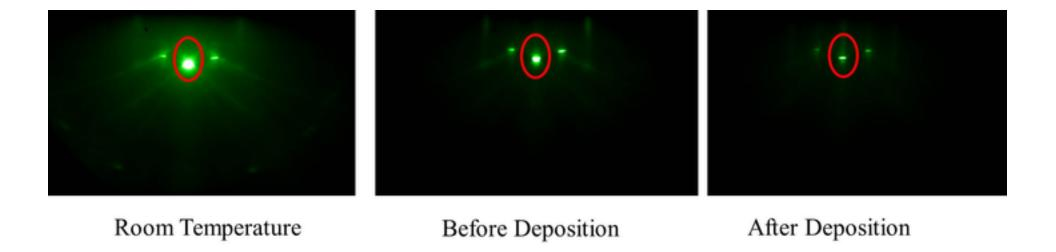
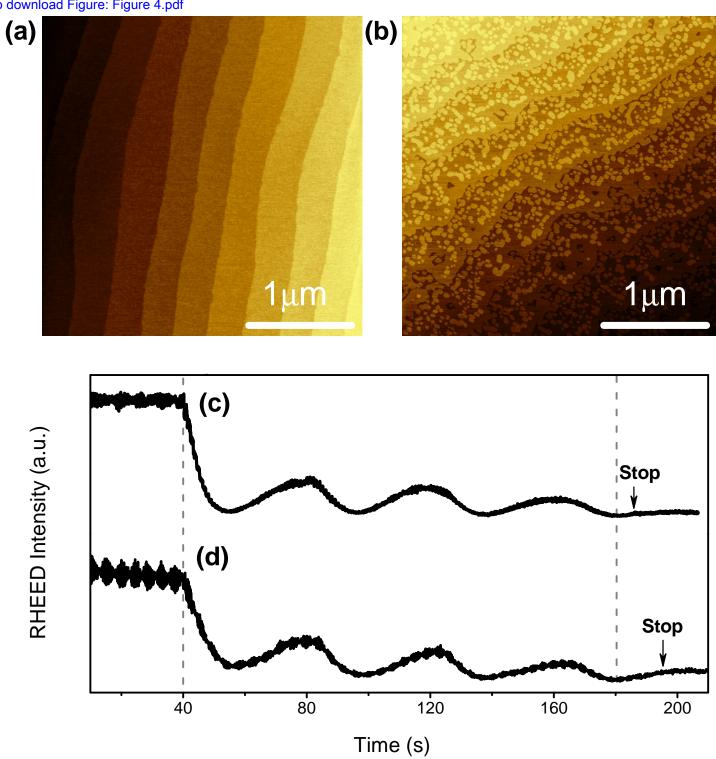
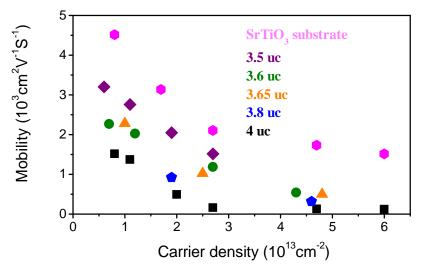


Figure 4 Click here to download Figure: Figure 4.pdf





Excel Spreadsheet- Table of Materials/Equipment
Click here to download Excel Spreadsheet- Table of Materials/Equipment: JoVE_Materials.xls

Name of Material/ Equipment	Company	Catalog Number	
(001) STO substrates	Crystec	NA	
LAO single crystal target	Crystec	NA	
Buffered HF solution	MicroChemicals	NA	
AIN sintered target	Kurt J. Lesker	EJTALNX282A4	
Photoresist	AZ Electronic Materials (Germany) GmbH	AZ5214	
PLD system	Neocera	NA	
PPMS system	Quantum Design	NA	
Kethely 2400 sourcemeter	Kethely	NA	
Photolithography mask aligner		NA	
Wire bonder	West Bond	7476D-79	

Comments/Description



1 Alewife Center #200 Cambridge, MA 02140 tel. 617.945.9051 www.jove.com

ARTICLE AND VIDEO LICENSE AGREEMENT

Title of Article: Author(s):	Controlled fractional unit cell growth of LaAlOs/SrTiOs interface near the critical Li, Changjian; Zeng, Shengwei; Lii, Weiming; Ariando; Venkatesan, T. and its scattering properties
ltem 1 (check or	ne box): The Author elects to have the Materials be made available (as described at w.jove.com/publish) via: Standard Access Open Access
Item 2 (check one	
	uthor is NOT a United States government employee.
	Author is a United States government employee and the Materials were prepared in the his or her duties as a United States government employee.
	uthor is a United States government employee but the Materials were NOT prepared in the his or her duties as a United States government employee.

ARTICLE AND VIDEO LICENSE AGREEMENT

- 1. Defined Terms. As used in this Article and Video License Agreement, the following terms shall have the following meanings: "Agreement" means this Article and Video License Agreement; "Article" means the article specified on the last page of this Agreement, including any associated materials such as texts, figures, tables, artwork, abstracts, or summaries contained therein; "Author" means the author who is a signatory to this Agreement; "Collective Work" means a work, such as a periodical issue, anthology or encyclopedia, in which the Materials in their entirety in unmodified form, along with a number of other contributions, constituting separate and independent works in themselves, are assembled into a collective whole; "CRC License" means the Creative Commons Attribution-Non Commercial-No Derivs 3.0 Unported Agreement, the terms and conditions of which can be found http://creativecommons.org/licenses/by-ncat: nd/3.0/legalcode; "Derivative Work" means a work based upon the Materials or upon the Materials and other preexisting works, such as a translation, musical arrangement, dramatization, fictionalization, motion picture version, sound recording, art reproduction, abridgment, condensation, or any other form in which the Materials may be recast, transformed, or adapted: "Institution" means the institution, listed on the last page of this Agreement, by which the Author was employed at the time of the creation of the Materials; "JoVE" means MyJove Corporation, a Massachusetts corporation and the publisher of The Journal of Visualized Experiments; "Materials" means the Article and / or the Video; "Parties" means the Author and JoVE; "Video" means any video(s) made by the Author, alone or in conjunction with any other parties, or by JoVE or its affiliates or agents, individually or in collaboration with the Author or any other parties, incorporating all or any portion of the Article, and in which the Author may or may not appear.
- 2. <u>Background</u>. The Author, who is the author of the Article, in order to ensure the dissemination and protection of the Article, desires to have the JoVE publish the Article and create and transmit videos based on the Article. In furtherance of such goals, the Parties desire to memorialize in this Agreement the respective rights of each Party in and to the Article and the Video.
- 3. Grant of Rights in Article. In consideration of JoVE agreeing to publish the Article, the Author hereby grants to JoVE, subject to Sections 4 and 7 below, the exclusive, royalty-free, perpetual (for the full term of copyright in the Article, including any extensions thereto) license (a) to publish, reproduce, distribute, display and store the Article in all forms, formats and media whether now known or hereafter developed (including without limitation in print, digital and electronic form) throughout the world, (b) to translate the Article into other languages, create adaptations, summaries or extracts of the Article or other Derivative Works (including, without limitation, the Video) or Collective Works based on all or any portion of the Article and exercise all of the rights set forth in (a) above in such translations, adaptations, summaries, extracts, Derivative Works or Collective Works and (c) to license others to do any or all of the above. The foregoing rights may be exercised in all media and formats, whether now known or hereafter devised, and include the right to make such modifications as are technically necessary to exercise the rights in other media and formats. If the "Open Access" box has been checked in Item 1 above, JoVE and the Author hereby grant to the public all such rights in the Article as provided in, but subject to all limitations and requirements set forth in, the CRC License.



1 Alewife Center #200 Cambridge, MA 02140 tel. 617.945.9051 www.jove.com

ARTICLE AND VIDEO LICENSE AGREEMENT

- 4. Retention of Rights in Article. Notwithstanding the exclusive license granted to JoVE in **Section 3** above, the Author shall, with respect to the Article, retain the non-exclusive right to use all or part of the Article for the non-commercial purpose of giving lectures, presentations or teaching classes, and to post a copy of the Article on the Institution's website or the Author's personal website, in each case provided that a link to the Article on the JoVE website is provided and notice of JoVE's copyright in the Article is included. All non-copyright intellectual property rights in and to the Article, such as patent rights, shall remain with the Author.
- 5. <u>Grant of Rights in Video Standard Access</u>. This **Section 5** applies if the "Standard Access" box has been checked in **Item 1** above or if no box has been checked in **Item 1** above. In consideration of JoVE agreeing to produce, display or otherwise assist with the Video, the Author hereby acknowledges and agrees that, Subject to **Section 7** below, JoVE is and shall be the sole and exclusive owner of all rights of any nature, including, without limitation, all copyrights, in and to the Video. To the extent that, by law, the Author is deemed, now or at any time in the future, to have any rights of any nature in or to the Video, the Author hereby disclaims all such rights and transfers all such rights to JoVE.
- 6. Grant of Rights in Video Open Access. This Section 6 applies only if the "Open Access" box has been checked in Item 1 above. In consideration of JoVE agreeing to produce, display or otherwise assist with the Video, the Author hereby grants to JoVE, subject to Section 7 below, the exclusive, royalty-free, perpetual (for the full term of copyright in the Article, including any extensions thereto) license (a) to publish, reproduce, distribute, display and store the Video in all forms, formats and media whether now known or hereafter developed (including without limitation in print, digital and electronic form) throughout the world, (b) to translate the Video into other languages, create adaptations, summaries or extracts of the Video or other Derivative Works or Collective Works based on all or any portion of the Video and exercise all of the rights set forth in (a) above in such translations, adaptations, summaries, extracts, Derivative Works or Collective Works and (c) to license others to do any or all of the above. The foregoing rights may be exercised in all media and formats, whether now known or hereafter devised, and include the right to make such modifications as are technically necessary to exercise the rights in other media and formats. For any Video to which this Section 6 is applicable, JoVE and the Author hereby grant to the public all such rights in the Video as provided in, but subject to all limitations and requirements set forth in, the CRC License.
- 7. Government Employees. If the Author is a United States government employee and the Article was prepared in the course of his or her duties as a United States government employee, as indicated in **Item 2** above, and any of the licenses or grants granted by the Author hereunder exceed the scope of the 17 U.S.C. 403, then the rights granted hereunder shall be limited to the maximum rights permitted under such

- statute. In such case, all provisions contained herein that are not in conflict with such statute shall remain in full force and effect, and all provisions contained herein that do so conflict shall be deemed to be amended so as to provide to JoVE the maximum rights permissible within such statute.
- 8. <u>Likeness, Privacy, Personality</u>. The Author hereby grants JoVE the right to use the Author's name, voice, likeness, picture, photograph, image, biography and performance in any way, commercial or otherwise, in connection with the Materials and the sale, promotion and distribution thereof. The Author hereby waives any and all rights he or she may have, relating to his or her appearance in the Video or otherwise relating to the Materials, under all applicable privacy, likeness, personality or similar laws.
- 9. Author Warranties. The Author represents and warrants that the Article is original, that it has not been published, that the copyright interest is owned by the Author (or, if more than one author is listed at the beginning of this Agreement, by such authors collectively) and has not been assigned, licensed, or otherwise transferred to any other party. The Author represents and warrants that the author(s) listed at the top of this Agreement are the only authors of the Materials. If more than one author is listed at the top of this Agreement and if any such author has not entered into a separate Article and Video License Agreement with JoVE relating to the Materials, the Author represents and warrants that the Author has been authorized by each of the other such authors to execute this Agreement on his or her behalf and to bind him or her with respect to the terms of this Agreement as if each of them had been a party hereto as an Author. The Author warrants that the use, reproduction, distribution, public or private performance or display, and/or modification of all or any portion of the Materials does not and will not violate, infringe and/or misappropriate the patent, trademark, intellectual property or other rights of any third party. The Author represents and warrants that it has and will continue to comply with all government, institutional and other regulations, including, without limitation all institutional, laboratory, hospital, ethical, human and animal treatment, privacy, and all other rules, regulations, laws, procedures or guidelines, applicable to the Materials, and that all research involving human and animal subjects has been approved by the Author's relevant institutional review board.
- 10. JoVE Discretion. If the Author requests the assistance of JoVE in producing the Video in the Author's facility, the Author shall ensure that the presence of JoVE employees, agents or independent contractors is in accordance with the relevant regulations of the Author's institution. If more than one author is listed at the beginning of this Agreement, JoVE may, in its sole discretion, elect not take any action with respect to the Article until such time as it has received complete, executed Article and Video License Agreements from each such author. JoVE reserves the right, in its absolute and sole discretion and without giving any reason therefore, to accept or decline any work submitted to JoVE. JoVE and its employees, agents and independent contractors shall have



ARTICLE AND VIDEO LICENSE AGREEMENT

full, unfettered access to the facilities of the Author or of the Author's institution as necessary to make the Video, whether actually published or not. JoVE has sole discretion as to the method of making and publishing the Materials, including, without limitation, to all decisions regarding editing, lighting, filming, timing of publication, if any, length, quality, content and the like.

11. Indemnification. The Author agrees to indemnify JoVE and/or its successors and assigns from and against any and all claims, costs, and expenses, including attorney's fees, arising out of any breach of any warranty or other representations contained herein. The Author further agrees to indemnify and hold harmless JoVE from and against any and all claims, costs, and expenses, including attorney's fees, resulting from the breach by the Author of any representation or warranty contained herein or from allegations or instances of violation of intellectual property rights, damage to the Author's or the Author's institution's facilities, fraud, libel, defamation, research, equipment, experiments, property damage, personal injury, violations of institutional, laboratory, hospital, ethical, human and animal treatment, privacy or other rules, regulations, laws, procedures or guidelines, liabilities and other losses or damages related in any way to the submission of work to JoVE, making of videos by JoVE, or publication in JoVE or elsewhere by JoVE. The Author shall be responsible for, and shall hold JoVE harmless from, damages caused by lack of sterilization, lack of cleanliness or by contamination due to the making of a video by JoVE its employees, agents or independent contractors. All sterilization, cleanliness or decontamination procedures shall be solely the responsibility of the Author and shall be undertaken at the Author's expense. All indemnifications provided herein shall include JoVE's attorney's fees and costs related to said losses or damages. Such indemnification and holding harmless shall include such losses or damages incurred by, or in connection with, acts or omissions of JoVE, its employees, agents or independent contractors.

- 12. Fees. To cover the cost incurred for publication, JoVE must receive payment before production and publication the Materials. Payment is due in 21 days of invoice. Should the Materials not be published due to an editorial or production decision, these funds will be returned to the Author. Withdrawal by the Author of any submitted Materials after final peer review approval will result in a US\$1,200 fee to cover pre-production expenses incurred by JoVE. If payment is not received by the completion of filming, production and publication of the Materials will be suspended until payment is received.
- 13. Transfer, Governing Law. This Agreement may be assigned by JoVE and shall inure to the benefits of any of JoVE's successors and assignees. This Agreement shall be governed and construed by the internal laws of the Commonwealth of Massachusetts without giving effect to any conflict of law provision thereunder. This Agreement may be executed in counterparts, each of which shall be deemed an original, but all of which together shall be deemed to me one and the same agreement. A signed copy of this Agreement delivered by facsimile, e-mail or other means of electronic transmission shall be deemed to have the same legal effect as delivery of an original signed copy of this Agreement.

A signed copy of this document must be sent with all new submissions. Only one Agreement required per submission.

CORRESPONDING AUTHOR:

Name:	Li, Changjian			
Department:	NUSNNI- Nano core			
Institution:	National University of Singapo			
Article Title:	Controlled fractional Unit cell growth of	[aA103/S	rTiO3 Interfaces near t	he critical thickness and
Signature:	li changian	Date:	12 March 2015	its scattering properties

Please submit a signed and dated copy of this license by one of the following three methods:

- 1) Upload a scanned copy of the document as a pfd on the JoVE submission site;
- 2) Fax the document to +1.866.381.2236;
- 3) Mail the document to JoVE / Attn: JoVE Editorial / 1 Alewife Center #200 / Cambridge, MA 02139

For questions, please email submissions@jove.com or call +1.617.945.9051

Response to Editorial comments:

The manuscript has been modified by the Science Editor to comply with the JoVE formatting standard. Please maintain the current formatting throughout the manuscript. The updated manuscript (53413_R4_051215.docx) is located in your Editorial Manager account. In the revised PDF submission, there is a hyperlink for downloading the .docx file. Please download the .docx file and use this updated version for any future revisions.

Changes made by the Science Editor:

1. There have been edits made to the manuscript.

Changes to be made by the Author(s):

- 1. Please revise the highlighting of the protocol to be 2.75 pages or less.
- 2. Grammar:

Please correct the grammar in the last sentence of the long abstract.

4.2 – Should be "using the same process as 3.2" rather than "using the same step." Also, do you mean 3.1 instead of 3.2?

First sentence, third paragraph of the discussion – "is a powerful" what? A word is missing.

3. Formatting:

Long abstract – Please define CMOS

1.5.2 – Please define rms.

For above comments, all changes have been made accordingly in the modified manuscript.

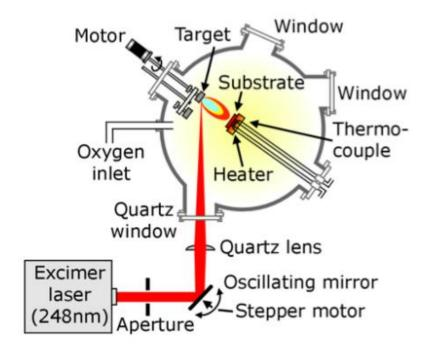
4. All figures should have a title and short description.

Figure caption serves the purpose, so no changes are made.

- 5. Additional detail is required:
- 3.1 How is the AlN target secured to the holder? What is the AlN target? Is this different from the STO and the substrate holder?
- 3.5 Is the substrate ablated by the laser? This is not clear.

To answer these two questions, I included a figure for PLD setup in figure R1. Hope this clears the doubts. The basic process is that: laser ablates the target (AlN and LAO in our case) surface, causing a small amount of target material to vaporize and expand towards to the substrate surface. Then the vaporized materials adsorb on substrate surface and grow into thin films. Whether thin film is crystalline or amorphous depends on the temperature of the substrate. In our study, AlN thin film is amorphous because it is deposited at room temperature while LAO is crystalline because of high temperature deposition.

PLD (Pulsed Laser Deposition)



Parameters

- Temperature
- Pressure
- •Target-to-Substrate Distance
- Substrate Material
- Laser Settings
 - Intensity
 - · # Pulses
 - Pulse Repetition
 Rate

(Adapted from http://www.coroflot.com/GideonGrossman/Thin-film-metal-oxide-solar-cells)

Figure R1 A schematic setup for PLD deposition.

4.5 – Which patter in figure 3 is the good one?

Figure 3 shows good RHEED patterns for different thin film growth states.

6.6 - How is this observed?

It is read through the multimeter which has the same connection for application of the gate bias.

6. References: Please abbreviate all journal titles.

Changes have been included in the modified manuscript.

Copyright clearance license (as requested by JoVE)
Click here to download Supplemental File (as requested by JoVE): Rightslink Printable License.pdf

Supplemental File (as requested by JoVE)
Click here to download Supplemental File (as requested by JoVE): 3.1Visual.png